

**Optical properties of irradiated imidazolium based room temperature ionic liquids: New
microscopic insights of the radiation induced mutations**

Apurav Guleria, Ajay K Singh and Soumyakanti Adhikari

Radiation & Photochemistry Division, Bhabha Atomic Research Centre, Mumbai 400 085, India

Correspondence E-mail: aguleria@barc.gov.in

Supporting Information

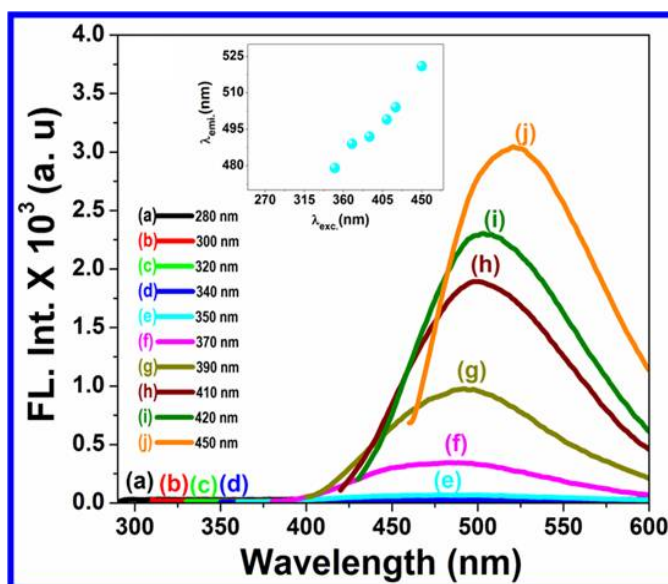


Fig.S1. Fluorescence (FL) spectra of neat FAP1 irradiated with an absorbed dose of 400kGy.

Inset: Plot of λ_{exc} vs. λ_{em} showing the shifts in the maximum intensity peak positions.

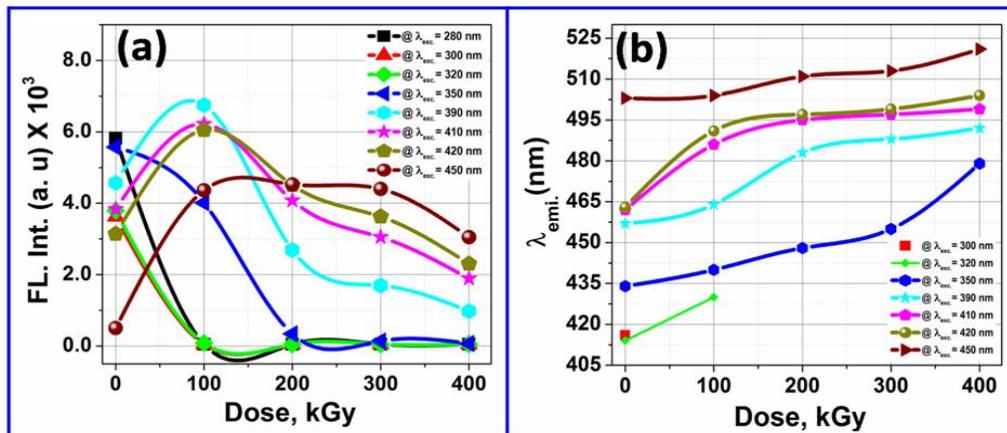


Fig.S2. Plots of FL intensity vs. dose (a) and λ_{em} vs. dose (b) for **FAP1** at different excitation wavelengths.

Table S1. Table showing the corresponding λ_{em} and maximum FL intensity values for neat pre and post irradiated **FAP1** at different $\lambda_{exc.}$ and absorbed dose values.

Dose $\lambda_{exc.}$ (nm)	0 kGy		100 kGy		200 kGy		300 kGy		400 kGy	
	λ_{em} (nm)	Max. Intensity								
280	332	5823	No emission	-						
300	416	3629	No emission	-						
320	414	3792	430	84	No emission	-	No emission	-	No emission	-
350	434	5574	440	4014	448	340	455	136	479	69
390	457	4572	464	6750	483	2689	488	1696	492	976
410	462	3835	486	6220	495	4047	497	3049	499	1890
420	463	3140	491	6050	497	4510	499	3625	504	2305
450	503	500	504	4360	511	4526	513	4400	521	3047

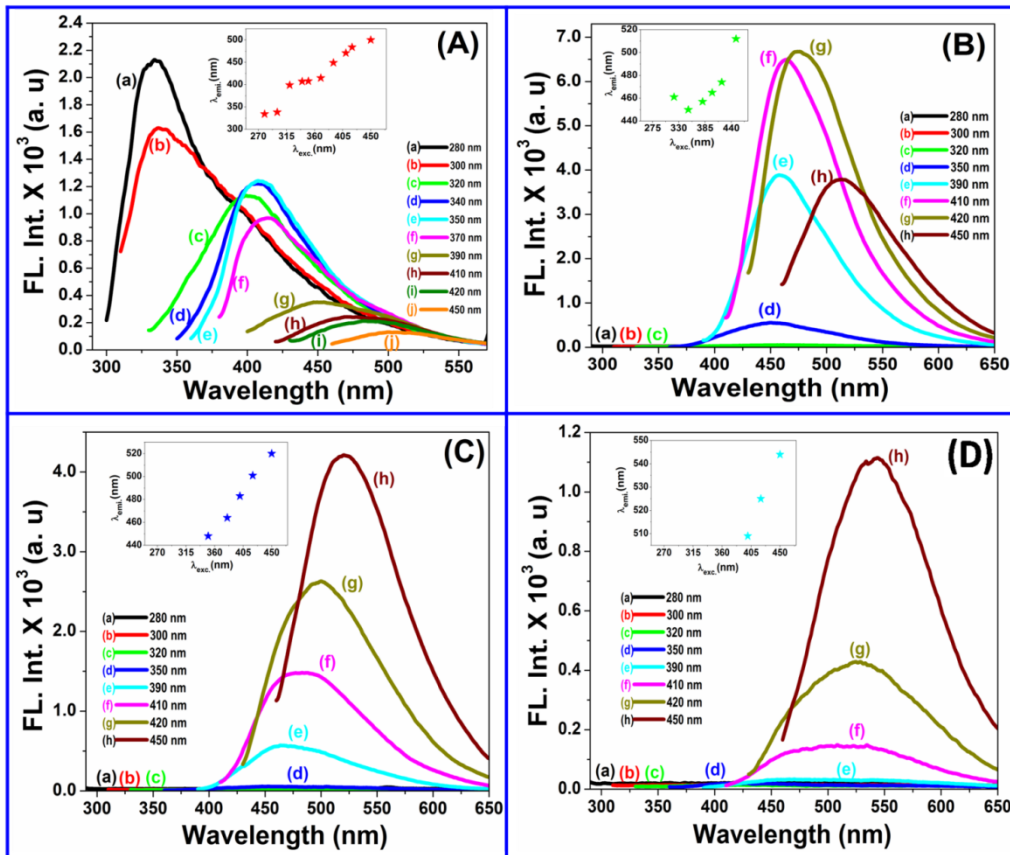


Fig.S3. FL spectra of neat unirradiated (A) and post irradiated **FAP2** at various radiation doses i.e. 100 kGy (B); 200 kGy (C); 300 kGy (D). Inset: Plot of λ_{exc} . vs. λ_{em} showing the shifts in the maximum intensity peak positions.

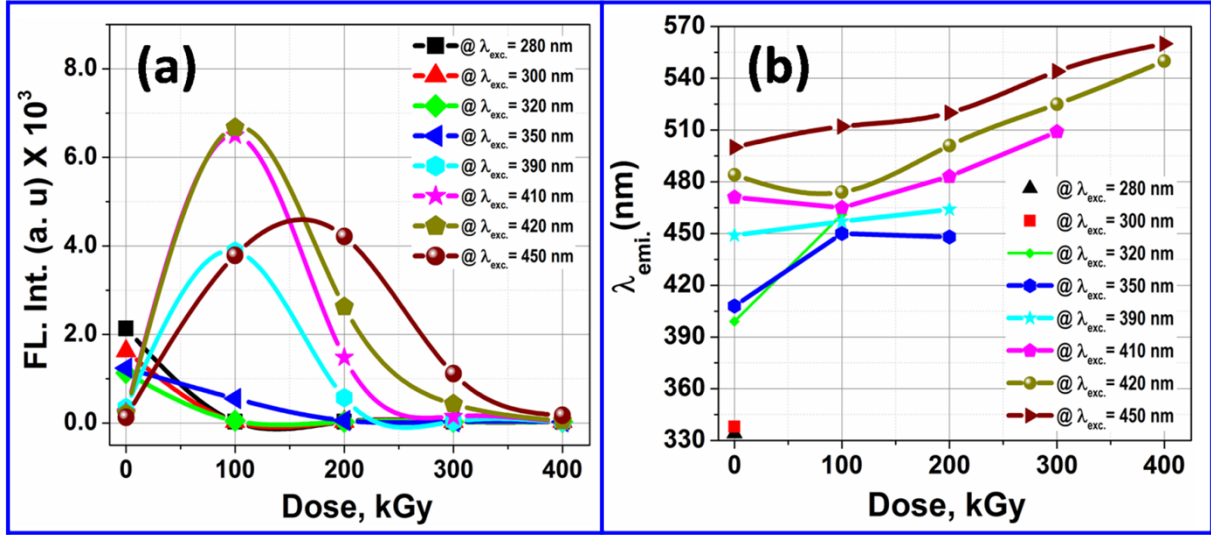


Fig.S4. Plots of FL intensity vs. dose (a) and λ_{em} vs. dose (b) for **FAP2** at different excitation wavelengths.

Table S2. Corresponding λ_{em} and maximum FL intensity values for pre- and post-irradiated **FAP2** at λ_{exc} and absorbed dose values.

Dose λ_{exc} (nm)	0 kGy		100 kGy		200 kGy		300 kGy		400 kGy	
	λ_{em} (nm)	Max. Intensity								
280	334	2135	No emission	-						
300	338	1626	No emission	-						
320	399	1134	461	51	No emission	-	No emission	-	No emission	-
350	408	1242	450	553	448	56	No emission	-	No emission	-
390	449	350	457	3886	464	572	No emission	-	No emission	-
410	471	243	465	6497	483	1482	509	148	No emission	-
420	484	213	474	6674	501	2626	525	429	550	50
450	500	130	512	3787	520	4214	544	1115	560	172

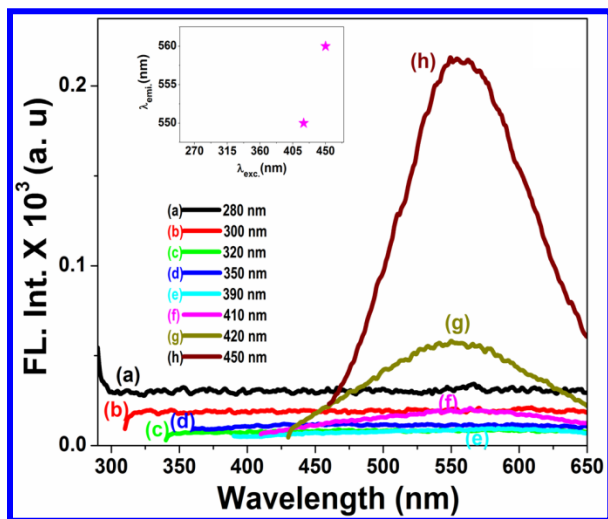


Fig.S5. FL spectra of neat **FAP2** irradiated with an absorbed dose of 400kGy. Inset: Plot of λ_{exc} vs. λ_{em} showing the shifts in the maximum intensity peak positions.

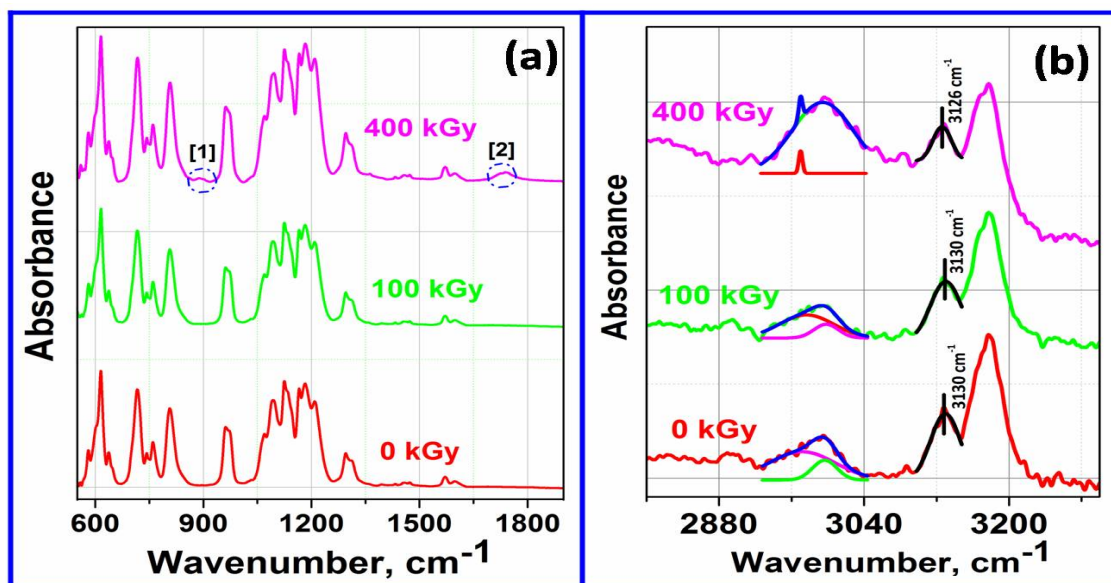


Fig.S6. FTIR spectra of neat pre- and post-irradiated **FAP1** at various radiation doses i.e. 0 kGy, 100 kGy and 400 kGy.

FTIR spectral analysis of pre- and post-irradiated FAP1 IL

Up to a dose of 100 kGy, no significant changes were observed in the FTIR spectra of irradiated ILs, which reflects their radiation stability. The intensity of the peaks in the region 1180-1220 cm^{-1} were found to increase on irradiation (for dose ≥ 100 kGy), which could be attributed to the formation of radiolytic products with $-\text{CF}_3$ units.¹⁻³ At the same time, some perturbations in the imidazolium ring and possible dissociation (or dislocations) of the alkyl groups attached to it were noticed from the decrease in the intensity of peaks located in the region 1400-1480 cm^{-1} on irradiation of IL. These peaks (at ~ 1433 cm^{-1} , ~ 1457 cm^{-1} and ~ 1463 cm^{-1}) originates due to the ring in-plane asymmetric stretching, (N)CH₃ CN stretching, (N)CH₃ HCH symmetric bending.³

⁴ Similar variations in the region 1400-1480 cm^{-1} were also observed in **FAP2**, when irradiated to high radiation doses. To precisely determine the changes in the C-H bond stretching frequencies of the ethyl and the terminal methyl group attached to the side chain of the imidazolium cation, a Gaussian peak fitting was carried out in the region 2900-3000 cm^{-1} and has been shown in the blue color in Fig.S6b. The peaks at ~ 2996 cm^{-1} accompanied by a shoulder peak at ~ 2972 cm^{-1} (assigned to Ethyl HCH symmetric stretching)⁴ were found to be broadened and red shifted by 2-3 cm^{-1} in post-irradiated **FAP1** (@ 400 kGy).

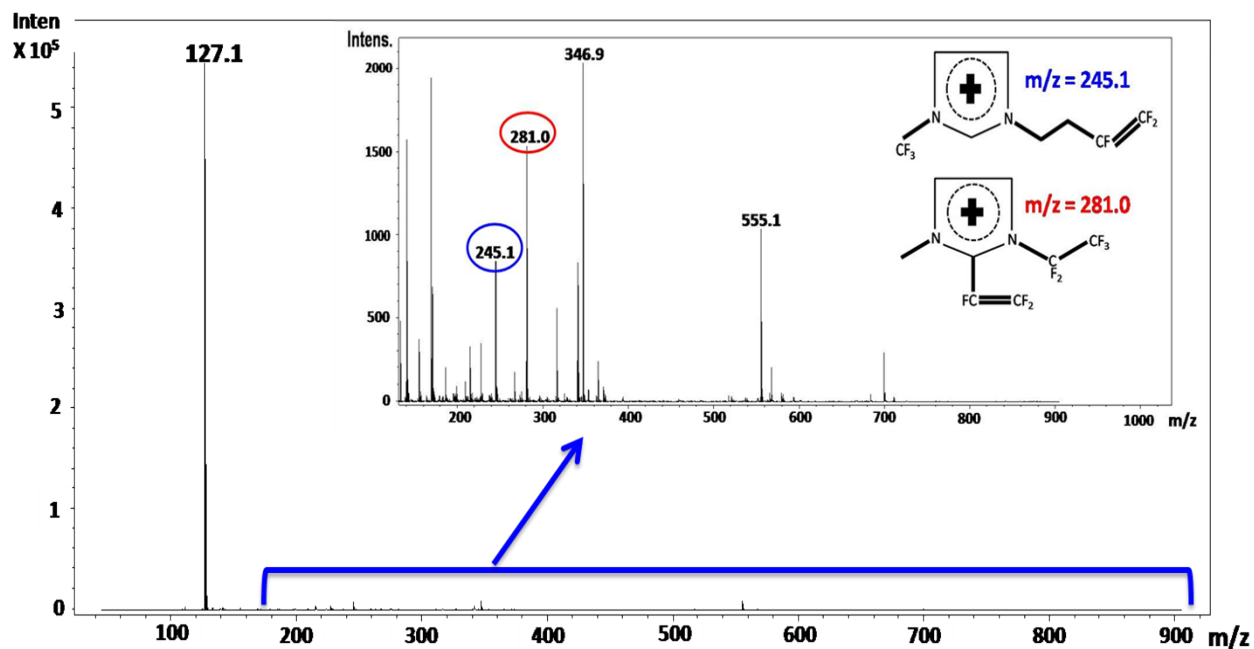


Fig.S7. ESI (+) mass spectrum of post-irradiated **FAP2** @ 100 kGy. The possible molecular structures of radiolytic products containing double bond units have been shown in the inset along with their m/z values.

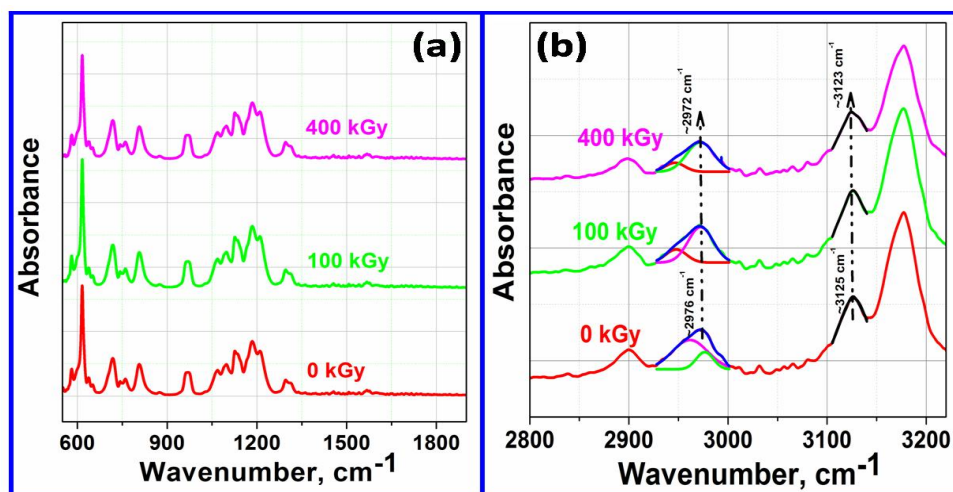


Fig.S8. FTIR spectra of neat unirradiated and post-irradiated **FAP2** at various radiation doses i.e. 0 kGy, 100 kGy and 400 kGy.

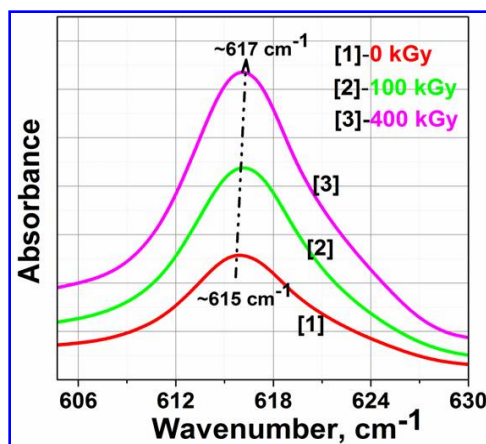


Fig.S9. FTIR spectra of neat unirradiated and post-irradiated **FAP2** at various radiation doses i.e. 0 kGy, 100 kGy and 400 kGy.

FTIR spectral analysis of pre- and post-irradiated FAP2 IL

The FTIR spectra of **FAP2** irradiated at different radiation doses (same as in case of **FAP1**) has been shown in Fig.S8. On careful evaluation of the spectra, some perturbations were noticed in the bonding interactions as well as their strengths, which have been discussed as follows. A blue shift in the peak frequency originated due to C-N stretching ($\sim 615 \text{ cm}^{-1}$)⁵ was observed (see Fig.S9). Analogous to **FAP1**, a broad peak in the range 1700-1750 cm^{-1} was observed in IR spectra of irradiated **FAP2** IL (not shown), which indicates the formation of radiolytic products with multiple bonding functional groups i.e. C=O, C=C, -CF=CF-, -CF=CF₂.⁶ Peak at $\sim 2976 \text{ cm}^{-1}$ representing the HCH stretching vibrations in the ethoxy group (attached to ring N)^{3, 4} of **FAP2** red shifted to $\sim 2972 \text{ cm}^{-1}$ on irradiation. Also, the peak at $\sim 3127 \text{ cm}^{-1}$ for the ring NC(H)NCH (or C₂-H)⁷ was found to be red shifted to 3123 cm^{-1} . The introduction of conjugation by the attachment of alkenyl groups (as mentioned in the main script) could also be one of the probable reasons behind the as observed red shift. In fact, the peaks corresponding to the formation of conjugated C=C groups were noticed in the Raman spectra of irradiated ILs (discussed in the manuscript).

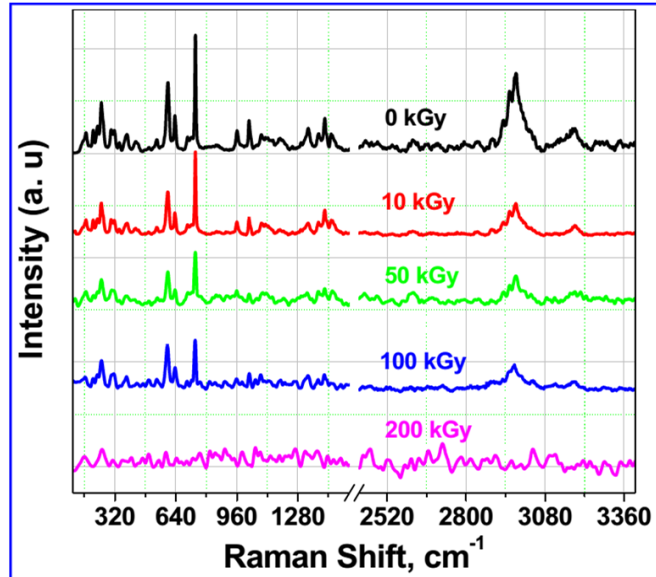


Fig.S10. Raman spectra of neat unirradiated and post irradiated **FAP1** at various radiation doses i.e. 0 kGy, 10 kGy, 50 kGy, 100 kGy and 200 kGy.

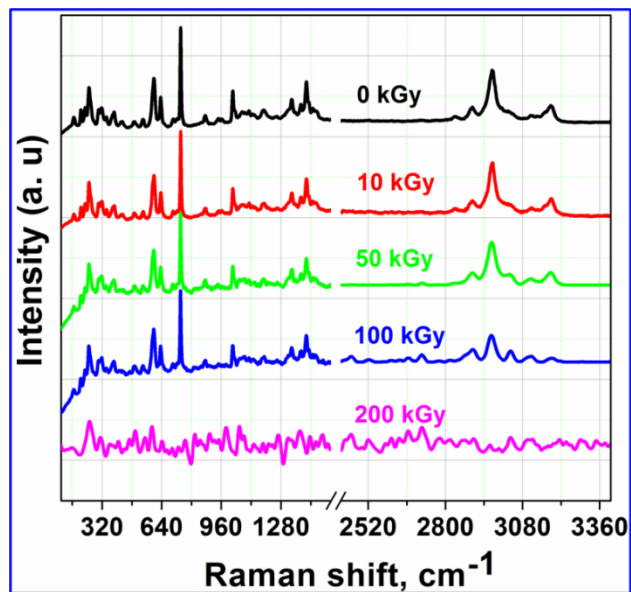


Fig.S11. Raman spectra of neat unirradiated and post irradiated **FAP2** at various radiation doses i.e. 0 kGy, 10 kGy, 50 kGy, 100 kGy and 200 kGy.

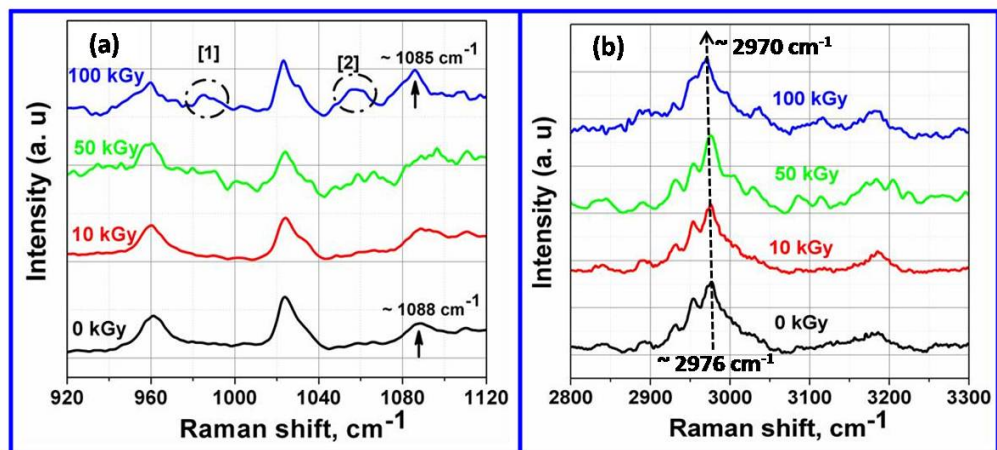


Fig.S12. Raman spectra of neat unirradiated and post-irradiated **FAP1** in different wave number regions at various radiation doses i.e. 0 kGy, 10 kGy, 50 kGy and 100 kGy.

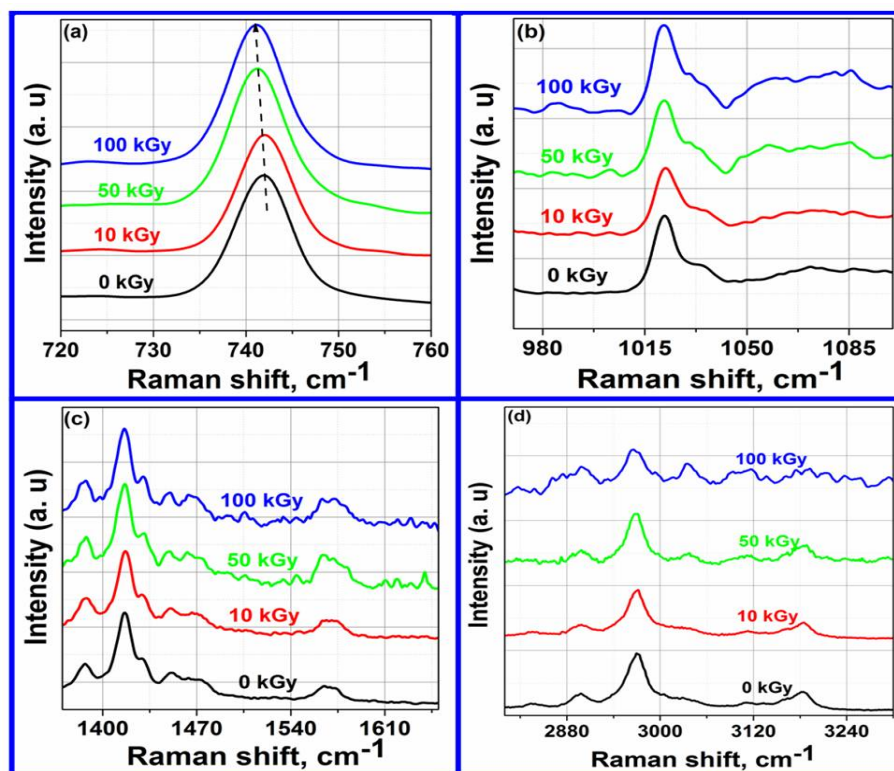


Fig.S13. Raman spectra of neat unirradiated and post-irradiated **FAP2** in different wave number regions at various radiation doses i.e. 0 kGy, 10 kGy, 50 kGy and 100 kGy.

Raman spectral analysis of pre- and post-irradiated FAP ILs

As can be seen, the Raman spectra of the ILs did not exhibit significant changes on irradiation up to a radiation dose of 100 kGy (see Fig.S10 & S11). However, at a radiation dose ≥ 200 kGy, the spectra appeared to vary considerably which in actual case is due to fluorescence (from the radiolytic products). The perturbations observed in the networking structure of **FAP1** and **FAP2** on irradiation has been explained as follows. A red shift was observed in the symmetric bending modes of $-\text{CF}_3$ (at $\sim 742 \text{ cm}^{-1}$) for **FAP2** on irradiation (see Fig.S13a). A broad peak centered at $\sim 985 \text{ cm}^{-1}$ emerges at a radiation dose ≥ 50 kGy (for both **FAP1** (Fig.S12a) and **FAP2** (Fig.S13b)), which indicates the formation of radiolytic products with vinyl C-H groups.⁸ While, broad peak marked as [2] ($1050\text{-}1070 \text{ cm}^{-1}$) in Fig.S12a is most plausibly attributed to the formation of fluoroalkanes.⁸ Besides, in-plane bending C-H vibrational frequency (in **FAP1**) at $\sim 1088 \text{ cm}^{-1}$ red shifted to 1085 cm^{-1} on irradiation at a radiation dose of 100 kGy.² Furthermore, red shifts in the frequencies representing ring in-plane asymmetric stretching, CC stretching, CH_3 (N) CN stretching (from 1421 cm^{-1} to 1419 cm^{-1}) and broadening in the CH_2 (N) CN stretching vibrations ($\sim 1570 \text{ cm}^{-1}$)³ was observed in Raman spectra of **FAP1** on irradiation. Similar distortions in the corresponding wavenumber regions were observed for post-irradiated **FAP2** (see Fig.S13). There have been additional strong evidences which indicate perturbations in the bonding interactions amongst the cationic and the anionic moieties and their surrounding environments. This could be observed primarily from the variations in the C-H stretching frequencies of the alkyl side chains in the region $2800\text{-}3200 \text{ cm}^{-1}$. For instance, in case of **FAP1**, peak most probably representing the ring CH_3 HCH symmetric stretching at $\sim 2932 \text{ cm}^{-1}$ red shifted to $\sim 2929 \text{ cm}^{-1}$ at high radiation dose of 100 kGy.⁴ Peak at $\sim 2953 \text{ cm}^{-1}$ could be assigned to CH_2 HCH stretching frequency⁴ was found to broaden at high radiation dose (see Fig.S12b),

and most possibly be attributed to the presence of radiolytic products with variations in the C-H bond strengths. Further, a red shift (from 2976 cm⁻¹ to 2970 cm⁻¹ @ 100 kGy) in the asymmetric stretching vibrational frequency of ethyl HCH was observed (in **FAP1**), which signifies the weakening of the respective bond strength.⁴ Similar red shift was observed (asymmetric stretching vibrational frequency of ethyl HCH) for irradiated **FAP2** (@ 100 kGy). Peak at ~ 3180 cm⁻¹ representing the ring HCCH symmetric stretching⁴ broadened at higher radiation doses in both the FAP ILs, which is a clear indication of the presence of radiolytic products derived from the imidazolium cation with varying bonding strengths.

Table S3. Lifetime values for post-irradiated **FAP1** and **FAP2** at various absorbed dose values. The values provided in the parentheses are the respective amplitudes for each times constants (T1, T2, and T3).

Sample	Dose	T1	T2	T3	χ^2	$\langle\tau\rangle$, ns
[EMIM][FAP]	0 kGy	2.47 ns (0.42)	9.02 ns (0.50)	0.42 ns (0.08)	1.09	5.58 ns
[EMIM][FAP]	100 kGy	3.40 ns (0.39)	9.84 ns (0.51)	0.95 ns (0.10)	1.08	6.43 ns
[EMIM][FAP]	200 kGy	3.40 ns (0.41)	9.87 ns (0.51)	0.88 ns (0.08)	1.08	6.49 ns
[EMIM][FAP]	400 kGy	3.48 ns (0.41)	10.2 ns (0.52)	0.92 ns (0.07)	1.03	6.79 ns
[EOHMIM][FAP]	0 kGy	3.14 ns (0.49)	9.93 ns (0.41)	0.76 ns (0.1)	1.03	5.68 ns
[EOHMIM][FAP]	100 kGy	4.25 ns (0.40)	11.3 ns (0.48)	1.35 ns (0.13)	1.05	7.29 ns
[EOHMIM][FAP]	200 kGy	3.86 ns (0.31)	10.0 ns (0.60)	1.19 ns (0.09)	1.06	7.30 ns

References

1. K. P. Huang, P. Lin and H. C. Shih, *J. Applied Phys.*, 2004, **96**, 354-360.
2. A. M. Moschovia, S. Ntaisb, V. Dracopoulosb and V. Nikolakis, *Vibrational Spectroscopy*, 2012, **63**, 350–359.
3. J. Kiefer, J. Fries and A. Leipertz, *Appl Spectrosc.*, 2007, **61**, 1306-1311.
4. N. E. Heimer, R. E. D. Sesto, Z. Meng, J. S. Wilkes and W. R. Carper, *Journal of Molecular Liquids*, 2006, **124**, 84 – 95.
5. N. R. Dhumal, H. J. Kim and J. Kiefer, *J. Phys. Chem. A*, 2011, **115**, 3551–3558.
6. (a) Q. T. Le, S. Naumov, T. Conard, A. Franquet, M. Müller, B. Beckhoff, C. Adelman, H. Struyf, S. D. Gendt, and M. R. Baklanov, *ECS J. Solid State Sci. Tech.*, 2013, **2**, N93-N98; (b) X. Gu, T. Nemoto, A. Teramoto, T. Ito and T. Ohmi, *J. Electrochemical Society*, 2009, **156**, H409-H415.
7. S. B. Dhiman, G. S. Goff, W. Runde and J. A. LaVerne, *J. Phys. Chem. B*, 2013, **117**, 6782–6788.
8. J. Coates, in *Encyclopedia of Analytical Chemistry*, ed. R. A. Meyers, John Wiley & Sons Ltd, Chichester, 2000, pp. 10815–10837; G. Socrates, *Infrared and Raman characteristic group frequencies: Tables and Charts*, John Wiley & Sons, 2004; L. J. Bellamy, *Infrared Spectra of Complex Molecules*, Chapman & Hall, New York, USA, Vol. 1, 1975.